coatings

MDPI

Review

Progress in Wear Resistant Materials for Total Hip Arthroplasty

Rohit Khanna [1,*], Joo L. Ong [2], Ebru Oral [3,4] and Roger J. Narayan [5]

1 Department of Mechanical Engineering, The University of Texas at San Antonio, San Antonio, TX 78249, USA
2 Department of Biomedical Engineering, The University of Texas at San Antonio, San Antonio, TX 78249, USA; Anson.Ong@utsa.edu
3 Harris Orthopaedic Laboratory, Massachusetts General Hospital, Boston, MA 02114, USA; EORAL@mgh.harvard.edu
4 Department of Orthopaedic Surgery, Harvard Medical School, Boston, MA 02115, USA
5 Joint Department of Biomedical Engineering, University of North Carolina and North Carolina State University, Raleigh, NC 27695, USA; Roger_Narayan@unc.edu
* Correspondence: rkhannaJP@gmail.com; Tel.: +1-210-458-5524

Received: 20 June 2017; Accepted: 5 July 2017; Published: 9 July 2017

Abstract: Current trends in total hip arthroplasty (THA) are to develop novel artificial hip joints with high wear resistance and mechanical reliability with a potential to last for at least 25–30 years for both young and old active patients. Currently used artificial hip joints are mainly composed of femoral head of monolithic alumina or alumina-zirconia composites articulating against cross-linked polyethylene liner of acetabular cup or Co-Cr alloy in a self-mated configuration. However, the possibility of fracture of ceramics or its composites, PE wear debris-induced osteolysis, and hypersensitivity issue due to metal ion release cannot be eliminated. In some cases, thin ultra-hard diamond-based, TiN coatings on Ti-6A-4V or thin zirconia layer on the Zr-Nb alloy have been fabricated to develop high wear resistant bearing surfaces. However, these coatings showed poor adhesion in tribological testing. To provide high wear resistance and mechanical reliability to femoral head, a new kind of ceramic/metal artificial hip joint hybrid was recently proposed in which 10–15 μm thick dense layer of pure α-alumina was formed onto Ti-6Al-4V alloy by deposition of Al metal layer by cold spraying or cold metal transfer methods with 1–2 μm thick Al_3Ti reaction layer formed at their interface to improve adhesion. An optimal micro-arc oxidation treatment transformed Al to dense α-alumina layer, which showed high Vickers hardness 1900 HV and good adhesion to the substrate. Further tribological and cytotoxicity analyses of these hybrids will determine their efficacy for potential use in THA.

Keywords: wear resistance; artificial hip joints; UHMWPE; ceramics; coatings; alumina/Ti alloy hybrid; cold spraying; cold metal transfer; micro-arc oxidation; total hip arthroplasty

1. Introduction

Every year more than one million hip and knee replacements are performed worldwide, which provide relief from pain, improved mobility, and better quality of life for patients. There will be an estimated 3.48 million knee replacements needed by 2030, an increase of approximately 673% as compared to the current number of procedures [1]. Artificial hip replacements are estimated to increase by 174% up from its current total procedures performed to 572,000 procedures per year in 2030. Current developments in the field of artificial hip joints are focused on the use of (a) short stems for minimal invasive surgery [2,3]; (b) new Ti alloys with better mechanical strength and biocompatibility than conventional Ti alloys [4–7]; (c) calcium phosphate coatings [8–12] or simple alkali and heat treatments

on the stem to provide bioactivity [13–17]; and (d) materials that impart better wear resistance and mechanical reliability on the articulating surfaces to minimize polyethylene wear debris-induced osteolysis [18–27]. Periprosthetic osteolysis is the primary cause of hip implant failure, which is the result of activation of an innate immune response caused by wear of bearing materials in total hip prostheses. Taken up by macrophages and multi-nucleated giant cells, the presence of wear debris particles may cause the release of cytokines, thereby resulting in inflammation that further activates osteoclasts at the interface between bone and implant and eventually leading to implant loosening and failure. One of the primary strategies to avoid implant revision is to eliminate the release of wear debris by improving the wear resistance and mechanical reliability of bearing couples that would ultimately enhance the longevity of the implant. Despite progressive attempts over last few decades, currently available hip replacement joints last only about 10–15 years. This relatively short implant life span is problematic for patients under 60 years; about 44% of this population demands a joint implant life expectancy of up to 20–25 years [28]. The demand for reliable hip joints is relatively high for young and active patients to maintain their work and life style comfortably. In this regard, this review is mainly focused on describing the evolution of materials and technologies developed to impart high wear resistance and reliability to bearing surfaces of artificial hip joints.

2. History of Development of Artificial Hip Joints

During 1955–1965, metal-on-metal (MoM) bearings were fabricated using large ball diameters (32 mm, 35 mm, and 41.5 mm). However, the use of MoM bearings declined in the 1970s for some years after Sir John Charnley introduced a total hip replacement (THR) device based on metal-on-polymer (MoP) composed of a small metal ball and a cemented polyethylene (PE) cup in 1963 [29]. Although this new tribocouple device received widespread acceptance, it was revealed over 6–8 years of clinical studies that implants with PE cups failed mainly due to osteolysis, a result of a destructive reaction by the body in the presence of PE wear debris [30]. Anticipating the issue of "polyethylene disease" or "cement disease", Pierre Boutin, a French surgeon, began implementing the use of alumina ceramic-on-ceramic (CoC) hip implants in clinical trials in the 1970s [31]. Since then, CoC devices have continuously been used in THA. These developments also made ceramic-on-polyethylene (CoP) combinations as competitive bearing alternative along with MoM and CoC over 1963–1973 period. Currently, the most frequently used artificial hip joints are composed of an acetabular cup, femoral head and stem, all of which are typically made of cast Cobalt-Chromium (Co-Cr) alloy. The lining of the acetabular cup is made of ultra-high molecular weight polyethylene (UHMWPE). Alternative materials are dense alumina ceramic and titanium−6% aluminum−4% vanadium (Ti-6Al-4V) alloys for the femoral head and the stem, respectively.

3. Ultra-High Molecular Weight Polyethylene

UHMWPE wear debris-mediated osteolysis is widely known as one of the most formidable challenges in hip arthroplasty [32,33]. To improve its wear resistance, UHMWPE is commonly exposed to irradiation at doses higher than that required for sterilization (40–100 kGy) to form cross-linked PE (XLPE) [34]. However, improvement of UHMWPE's wear resistance comes at the cost of reducing its ultimate tensile strength as a result of reduced ductility [35]. In addition, many of its mechanical properties are sensitive to oxidation [36,37], which is mainly due to the reactions of residual free radicals caused by irradiation and trapped in the material for prolonged periods of time [38,39]. Oxidative changes gradually decrease the polymer's molecular weight and affect its clinical performance through structural changes [40]. To overcome these problems, XLPE is stabilized by post re-melting or annealing and by the addition of antioxidants such as vitamin E to eliminate, reduce, or stabilize free radicals, with the intention of increased wear resistance as well as reduced potential for oxidation as compared to conventional XLPEs [18,19,41]. While some highly cross-linked UHMWPEs show higher oxidation *in vivo* than others [42], radiation cross-linking of UHMWPE has tremendously decreased (87%) the

incidence of wear particle-induced osteolysis in the first ten years of clinical use [43], especially in hips where wear damage is prominent.

In addition to state-of the art technology incorporating antioxidants for long-term stability [44–46], a recent application of a surface treatment on the XLPE articulating surface has improved the wear resistance by covering its surface with a thin layer (100–200 nm) of chemically-bonded Poly(2-methacryloyloxyethyl phosphorylcholine) (PMPC), which is formed by photo-induced graft polymerization; this material creates a super-lubricious layer that mimics articular cartilage [20]. A recent hip simulator study reported that MPC polymer grafted on the XLPE surface dramatically reduced the wear up to 70 million cycles [47]. Wear debris induced osteolysis and inflammatory responses may be suppressed by this new design of PMPC-grafted XLPE, which is attributed to the bio-inertness of bio-inspired MPC polymers [47]. Although this kind of artificial hip joint has been implanted in more than 20,000 patients since 2011 in Japan [47], it is a new technology whose success and impact will be determined in the longer term. Analysis of retrieved components and radiographic follow-up of patients [48] will continue to inform us on the effects of wear on future clinical performance.

4. Metallic Materials

Metallic materials such as cobalt-chromium-molybdenum (Co-Cr-Mo) and Ti alloys are commonly used in THA due to their superior mechanical strength, fracture toughness and ductility. Typically, CoCrMo alloys and Ti alloys are used as stem of artificial hip joints. Co-Cr alloy used as head in MoM artificial hip joint model has demonstrated mechanical reliability due to high mechanical strength and fracture toughness, but it tends to produce metal debris over the long-term, releasing metal ions that cause inflammation and blackening of periprosthetic tissue termed as metallosis. Incidents of metal sensitivity were reported to affect 10%–15% of the general population [49–51] and were higher among patients with failed joints. Ti-6Al-4V alloy is the most commonly used alloy for stem and acetabular cementless components of THR due to its low density, high mechanical strength, excellent corrosion resistance, and biocompatibility with bone [52]. Compared with Co-Cr alloys, the elastic modulus of 110 GPa for Ti alloy offers a more physiologically uniform stress distribution at the bone-implant interface. However, the release of potentially harmful metal ions such as aluminum (Al) and vanadium (V) from the Ti alloy has been reported to be associated with long term health problems such as peripheral neuropathy, osteomalacia and Alzheimer's disease [53,54].

Over the last few decades, vanadium-free Ti implants such as α + β Ti-6Al-7Nb alloy (ISO 5832-11), near β alloys such as Ti-13Nb-13Zr alloy (ASTM F1713-96), Ti-12Mo-6Zr-2Fe alloy (ASTM F1813-97) with improved biocompatibility have been developed by incorporating biocompatible elements such as Ta, Zr or Nb [4–7]. Metastable β type Ti-15Mo-5Zr-3Al and α + β type Ti-6Al-2Nb-1Ta alloys have been clinically developed for both cemented and cementless types of artificial hip joints. A new Ti-15Zr-4Nb-4Ta alloy with excellent mechanical properties and biocompatibility has been developed for artificial hip joint application [7]. To overcome stress shielding effects, recent research on Ti alloy development is focused on controlling processing to reduce the elastic modulus while retaining high biocompatibility and mechanical strength. In this regard, a metastable β type Ti alloy such as Ti-35Nb-7Zr-5Ta alloys with an elastic modulus of 55 GPa has been developed [55]. Nevertheless, Ti alloys are not used for manufacturing of femoral head due to their poor wear resistance. To overcome this issue, thermal oxidation treatments have been applied to Ti alloy to form oxides to improve surface hardness [56,57], laser surface treatments to alter its surface microstructures [58] and/or friction stir processing to change its metallic properties through localized plastic deformation [59]. However, these treatments do not provide superior wear resistance, which limit their use as the bearing surfaces of artificial hip joints.

5. Ceramics

5.1. Alumina

Alumina ceramics are most widely used in THA as femoral heads due to their bio-inertness, high wear resistance, and chemical durability. In terms of design, the surface finish of materials used for manufacturing of femoral heads or cups is an important requirement. Advances in alumina processing have revealed that an excellent surface finish can be achieved using high purity alumina with <0.5 wt % magnesium oxide as a sintering aid and compaction using hot-isostatic pressing before sintering to obtain a dense microstructure of fine-grained pure α-alumina with improved mechanical properties. As per ASTM F603, medical grade alumina for orthopedic implant use should have a bulk density of >3.94 gm/cc, grain size of <4.5 μm, and flexural strength of >400 MPa. Compared with MoP, artificial hip joints with CoP couple have shown 25%–30% reduction in wear rate in hip simulator and clinical studies [60,61]. Using an alumina-on-alumina couple, wear in THA was the lowest (0.01–0.1 mm^3/million cycles) as compared with MoP, CoP or MoM combinations [61,62]. Since its inception by Boutin in the 1970s, more than 2.5 million femoral heads of alumina and 100,000 liners have been implanted worldwide. Although incidences of fracture of alumina ceramics in THA are rare (0.14% reported in the USA in the mid-1990s), the uncertainty about risk of brittle fracture, rim chipping, squeaking [63] (audible noise) and stripe wear [64,65] in artificial hip joints with alumina CoC couple are mainly due to improper positioning [66] and cannot be eliminated. Squeaking in THA articulations with alumina CoC have been reported especially in some young patients, aged forty or under, despite high survivorship up to 97.4% at ten years [67,68]. Squeaking can be associated with impingement of femoral neck on the rim of the ceramic cup, due to difference in diameters of femoral heads, edge loading effect due to improper positioning during surgery or could also be due to micro-separation between femoral head and liner of cup, all of which increase friction in case of CoC bearing couples and hip dislocation and potentially lead to to revision of surgery. Current trends to increase the diameters of ceramic balls to 32 mm, 36 mm, or larger tend to make a positive effect. Nevertheless, the risk of catastrophic fracture of alumina cannot be eliminated.

5.2. Zirconia

To improve the mechanical reliability of the head, partially stabilized zirconia and yttria-stabilized tetragonal zirconia polycrystal (Y-TZP) ceramic with almost double fracture toughness of 6–10 MPa $\sqrt{m}$ and flexural strength of 1000 MPa than alumina, were introduced as alternatives in the 1980s. Improved mechanical properties in zirconia are attributed to stress-induced transformation toughening mechanism. Briefly, as crack propagates, zirconia undergoes phase transformation from tetragonal to monoclinic in leading to 3%–4% volume expansion in the zirconia grains, resulting in compressive stress to slow or arrest the crack, thereby increasing the toughness. Despite some good clinical results with seven-year [69] and ten-year [70] follow up, several controversial hip simulator and clinical reports have been published over 15 years of its clinical use in patients [71,72]. Unfortunately, a worldwide recall concluded in 2001 led to a sudden halt of manufacturing and clinical use of zirconia after many zirconia heads manufactured by St. Gobain were fractured *in vivo* due to change in sintering procedure. Even though transformation toughening led to high strength and toughness of designed Y-TZP heads, the spontaneous transformation to monoclinic polymorph in the presence of body fluid results in roughening and micro-crack formation on the surface of the head, thereby enhancing wear and eventual fracture as reported in *in vivo* studies [72]. This phenomenon is often referred as low-temperature hydrothermal aging. Close examinations of more than 100 retrieved Zr femoral heads revealed extensive cratering in addition to considerable monoclinic phase [71]. Further, eight and nine-year follow up revealed up to 85% monoclinic phase and dramatically higher surface roughness of up to 250 nm on the Prozyr heads retrieved from Sydney [73,74]. These critical issues almost restricted the use of Zr femoral heads in the US and EU markets. Although zirconia is commonly used in dentistry due to its aesthetics and high mechanical properties, its microstructure and processing

steps must be carefully examined before use. Hydrothermal aging is the Achilles' heel of zirconia, limiting its longevity.

5.3. Silicon Nitride

Silicon nitride is a non-oxide ceramic material with high strength and toughness and has been used as bearings, turbine blades for more than 50 years. In the medical field, it has been used in cervical spacer and spinal fusion devices [75] since 2008, with few adverse reports among 25,000 implanted spinal cages [76]. Silicon nitride has been recently considered as a bearing material in artificial hip and knee replacements due to its high biocompatibility, moderate Vickers hardness of 12–13 GPa, Young's modulus of 300 GPa, high fracture toughness of 10–12 MPa $\sqrt{m}$ and flexural strength of 1 GPa, with a typical grain size of 0.6 μm after alloying with small amounts of yttria and alumina [77]. The exceptional strength and toughness of silicon nitride are derived from its asymmetric needle-like interlocking grains surrounded by thin glassy phase at the grain boundary, which dissipates energy as crack propagates [78]. Silicon nitride has also been used as wear resistant coating by PVD or CVD methods [79,80]. However, coatings are non-stoichiometric, not fully crystalline, and do not resemble similar strength and toughness as polycrystalline materials, which limited their use as coatings for implants. Bulk silicon nitrides in articulation against itself and Co-Cr materials have shown wear rates that are comparable to those of alumina-on-alumina couple, which are the lowest among currently used bearing couples [81]. A recent hip simulator study indicated that self-mated silicon nitride couples have comparable wear performance to that of self-mated alumina up to three million cycles; however, some self-mated silicon nitride couples showed increased wear at the end of five million cycles as compared to alumina CoC [82]. This transition in wear regime from fluid film to lubrication was attributed to the formation and disruption of tribochemical film composed of a gelatinous silicic acid. Silicon nitrides articulating against PE or XLPE revealed similar wear performance as that of CoCr or alumina heads. There is some discrepancy between the hip simulator and *in vivo* studies for some femoral heads, further long-term clinical studies of retrieved heads of silicon nitride and hip simulator studies by others might be necessary before confirming the potential use of silicon nitride as bearing material for hip replacements.

5.4. Alumina-Zirconia Composites

Despite the long clinical history of alumina and zirconia in THR, both materials pose potential drawbacks. Attempts to overcome these material's weaknesses by combining alumina's hardness with zirconia's toughness led to the development of zirconia-toughened alumina (ZTA), which was first commercialized by CeramTec under the trade name of BIOLOX® Delta in around 2000. ZTA is an alumina matrix composite containing 75% fine grained alumina of 0.5–0.6 μm in diameter and 25% Y-TZP with a grain size of 1 μm or smaller to obtain a flexural strength of 1200 MPa and a fracture toughness of 6.5 MPa $\sqrt{m}$. The flexural strength and fracture toughness of ZTA are significantly higher than that of alumina while retaining superior chemical and hydrothermal stability like alumina. Superior mechanical strength and toughness of ZTA is attributed to the stress-induced transformation toughening mechanism offered by an optimal amount of fine grained zirconia dispersed throughout the ZTA microstructure. Additional toughening to alumina is provided by crack deflection at the boundaries of platelet-like alumina grains with magneto plumbite structure that are formed by solid solutions with a small amount of SrO and Cr_2O_3 additives during high temperature sintering.

This unique combination of transformation toughening and crack deflection mechanisms provides exceptional durability to BIOLOX® delta, which is not achieved by any other ceramic material used in the body. Addition of alumina to zirconia slows down the kinetics of hydrothermal ageing, which is a potential advantage over monolithic zirconia. Laboratory hip simulator wear tests on ZTA-on-ZTA couple revealed that the wear performance of ZTA CoC was better than that of alumina CoC [83]. Moreover, more strip wear was revealed on alumina CoC as compared with ZTA CoC tested under same tribological parameters. However, up to 30% monoclinic zirconia was detected on the surface of

ZTA, which shows that transformation from tetragonal to monoclinic zirconia happened during the articulation between ZTA cup and the ball [84]. *In vivo* wear results are more realistic as compared to hip wear simulator results. Even though BIOLOX delta components are clinically used for more than 12 years and have been implanted in more than six million patients, according to CeramTec company web information, longer term clinical reports will determine the efficacy of this new ceramic composite for long lasting hip prostheses.

Alumina toughened zirconia (ATZ) is another alumina-zirconia composite bearing material containing 80% Y-TZP and 20% alumina, which was developed and manufactured as Ceramys® by Mathys Orthopedics [85] in Germany in 2010. ATZ Ceramys is composed of 61% tetragonal zirconia, 17% cubic zirconia, 1% monoclinic zirconia and remaining alumina which form a fine-grained alumina dispersed in the zirconia matrix with average grain size of 0.4 μm for both zirconia and alumina. ATZ revealed a high flexural strength of more than 1200 MPa, a moderate hardness of 1500 HV, and a fracture toughness of 7.4 MPa $\sqrt{m}$ [23]. In addition, ATZ is reported to have improved wear performance with a wear rate of 0.06 mm^3/million cycles as compared with the 0.74 mm^3/million cycles for monolithic alumina heads in CoC configuration [24]. In addition to the critical hydrothermal aging effect of zirconia, there remain major concerns with the variation in manufacturing steps of zirconia-based materials by different manufacturers, which needs to be carefully assessed every time before implantation in the human body. Nevertheless, even composite ceramics are brittle and liable to fracture.

6. Ultra-Hard Coatings on Metals

To maintain the active lifestyle of patients requiring hip replacements, reliable designs of artificial hip joints with high wear resistance and mechanical reliability are needed to extend their current life span from 10–15 years to 25–30 years, which otherwise will require multiple revision surgeries that will burden healthcare expenditure all over the world. The dire need to produce more durable artificial joints is made explicit by the fact that hip and knee replacement surgeries have increased by 20% during the last five years [86]. Trends for revision surgeries are becoming more common among young and active patients aged between 45 and 64 who will require functional artificial hip for at least 30 years [86] to maintain their active lifestyle. While Co-Cr alloy in self-mated configuration or the alloy heads sliding against PE or XLPE are frequently used in THA, over 50% artificial hip joints fail mainly due to osteolysis-mediated aseptic loosening in addition to metal ion allergies over a long-term period [87]. A frequently used alternative hybrid approach is to coat the metallic alloys with ultra-hard and biocompatible surface layers such as diamond-like carbon (DLC; 5000 HV) [88] or titanium nitride (TiN 2100 HV) [89]. This approach ensures that the original properties of high strength metallic substrate are retained while: (a) supporting a bearing surface; and (b) avoiding the release of toxic metal ions from the underlying the Ti alloy substrate. The release of wear debris from TiN-coated Ti alloy after delamination enhanced wear by third-body wear mechanisms *in vivo* [89]. DLC-coated Ti-6Al-4V alloy showed numerous pits, local delamination, and crevice corrosion while articulating against PE and showed only 54% survival rate after 8.5 years of clinical study [90]. To improve the adhesion between the coating and the substrate, interlayers of Ti, tantalum (Ta), or CrC have been used to minimize the residual stresses at the interface. Recently, a DLC layer with a varying thickness of multi-interlayers of Cr-Cr_2N was reported to increase the fracture strength or adhesion of the DLC coating [91]. However, the hardness of these multilayer coatings (800–1000 HV) was almost half of that of sintered alumina (1800–2000 HV) [91]. In addition, there could be concerns about inflammation due to release of Cr over the long term.

Another method is to deposit pure diamond on the metal heads. In this regard, coatings of ultra-nanocrystalline diamond (UND) with a grain size of 3–100 nm have been applied directly to Ti and Co-Cr alloys using microwave plasma CVD [92,93]. UND coatings possess high hardness (56–80 GPa) and low surface roughness, RMS value < 10 nm, that is shown to provide high wear resistance to third-body wear particles [94]. These coatings have been applied to Ti and its alloys;

good corrosion resistance, adhesion, and toughness have been reported in addition to comparable tribological performance to those of MoM, MoP and CoC couples, which makes them suitable for THA application [95]. However, large compressive stresses are retained within the UND coatings due to impurities at their grain boundaries, which affected their adhesion with the substrate [96]. Further improvements in processing parameters are needed to avoid the risk of delamination of the UND coatings, which will govern their clinical use. In a nutshell, further improvements are needed in these coating technologies to meet high wear resistance, mechanical reliability and adhesion requirements for long lasting total hip prostheses.

7. Hybrid Design of Oxide Ceramic Layer on Metal: Oxinium™

A promising approach of a dense oxide layer on metal substrate combines high mechanical strength and toughness of underlying metal with advantages of an oxide layer with bio-inertness, high corrosion and wear resistance as an articulating surface. If native TiO_2 layer on the surface of high mechanical strength Ti alloys was at least a few microns thick and wear resistant for long lasting hip prostheses or bulk ceramics were not inherently brittle, there could have been no interventions to deposit alternative wear resistant materials on metals over the last few decades. These drawbacks have spurred alternative explorations of bio-inert oxide ceramic layers on metallic substrates, adopting a hybrid approach by wedding the superior wear resistance of ceramics with the superior toughness of metals.

A layer of monoclinic zirconia 5 μm thick formed on the surface of Zr-2.5% Nb alloy by heat treatment of the alloy at 500 °C [25] has been successfully applied to a femoral head commercialized as Oxinium™ (OxZr; Smith & Nephew, Memphis, TN, USA). OxZr is not a coating, but a surface transformed layer formed by oxygen diffusion hardening treatment, which is expected to provide improved resistance under load bearing operations. Compared to monolithic zirconia, thin zirconia layer on the Zr-Nb alloy avoids catastrophic failure of the implant. *In vitro* hip simulator studies have shown remarkable reductions in wear of OxZr by 45% articulating against XLPE for total hip and knee arthroplasty as compared with Co-Cr alloys [26,97]. Although OxZr heads are being routinely used for young and active patients, some clinical studies have reported extensive damage of OxZr heads articulating against XLPE [98,99], indicating poor mechanical reliability of the joint. Moreover, OxZr head has only 5 μm thick layer of zirconia formed on the Zr-Nb alloy, which is not expected to last up to 25–30 years to meet the demands of durable artificial hip joints that are needed for patients aged 40 or younger. OxZr is still in clinical use; receipients of OxZr implants will need to undergo regular check-up to ensure the good condition of implants in their bodies. From the materials design perspective, it is intriguing to reveal the reasons for the good adhesion between OxZr layer and the metal substrate given that they are incompatible materials due to significant differences in their physical, chemical and mechanical properties. However, this information is not clarified in the literature yet despite more than eight years of clinical use of OxZr heads. The ideal design of a strong interface between ceramic and metal is not revealed yet and is a fundamental gap in the knowledge. Once this gap is filled, it would lead to new knowledge in terms of methodologies that are needed for designing reliable artificial hips with an extended lifespan of more than 25–30 years.

8. Rationale for Design of New Kind of Ceramic/Metal Hybrid Artificial Joint

With increasing aging population and demands for active and young patients aged 40 and under, the life span of artificial joints is expected to be more than 25–30 years. To meet these demands, the focus is to design and develop new kinds of artificial joints with high wear resistance and mechanical reliability.

8.1. Selection and Design of Materials

Materials used to design future generation durable femoral head or cup made of ceramic/metal hybrids should meet demands of high wear resistance at bearing surface, supported by a metallic

material that can sustain high toughness. These demands have not been met by any of the currently used materials for artificial joints including Oxinium™, as discussed in Section 7. To meet these demands, a promising ceramic/metal hybrid design was recently proposed [100–103] in which better wear resistance might be obtained if zirconia is replaced with the alumina as an articulating surface because the latter has higher hardness. Mechanical reliability of articulating surface might increase if Zr-Nb alloy substrate is replaced by Ti-6Al-4V alloy because the latter has higher mechanical strength and fracture toughness than that of the former or Co-Cr alloy, commonly used as the head in THA. Furthermore, alumina layer formed on the tough Ti alloy is expected to offer better mechanical reliability as compared with monolithic alumina that is liable to catastrophic fracture. In addition, alumina shows better long-term *in vivo* stability than zirconia. Oxinium™ is composed of only 5 μm thick layer of monolithic zirconia on the Zr-Nb alloy. Therefore, formation of dense α-alumina layer with thickness of 5 μm or more is expected to last longer than Oxinium™. In addition to requirement for high wear resistance, a good adhesion between alumina layer and the Ti alloy is critical for reliability of alumina/Ti alloy hybrid for efficient load transfer mechanism during operations of artificial hip.

It is technically challenging to fabricate dense and pure α-alumina layer on the Ti alloy given that alumina and the Ti alloy are very incompatible with each other due to significant differences in their coefficient of thermal expansion (α_{Alumina} = 7.5 × 10^{-6}/K and $\alpha_{\text{Ti-6Al-4V}}$ = 9.1–9.8 × 10^{-6}/K) and mechanical properties (Hardness, H_{Alumina} = 2100 HV, $H_{\text{Ti alloy}}$ = 350 HV; fracture toughness, $K_{\text{Ic,Alumina}}$ = 3–4 MPa $\sqrt{\text{m}}$, $K_{\text{Ic,Ti alloy}}$ = 75 MPa $\sqrt{\text{m}}$), which could result in the residual stresses at the interface between them. High residual stresses could lead to cracks at the interface and subsequent delamination of alumina layer. Although the ideal design of strong interface between ceramic and metal is not fully revealed yet, it was recently proposed that formation of an intermediate AlTi type of bonding layer with metallurgical bond-like characteristics might tend to minimize the residual stresses at alumina-Ti interface and could also enhance the mechanical reliability of the joint as well [100–103]. The cross-sectional view of newly proposed alumina/Ti alloy hybrid (ATH) artificial hip joint model is shown schematically in Figure 1a. This kind of designed hybrid could be used for both the cup and head in alumina-on-alumina type of contact configuration, as shown in Figure 1b. The rationale behind this configuration is that alumina CoC combination has shown lowest wear rate (0.01 mm^3/million cycles) among the currently used materials in THA. Hence, it is expected that wear of ATH-on-ATH could be similar as well. Compared with monolithic alumina, ATH design could offer better mechanical reliability to artificial hip since bearing surface is supported by tough Ti alloy. The proposed ATH head could also be used in articulation against conventional PE or XLPE liner.

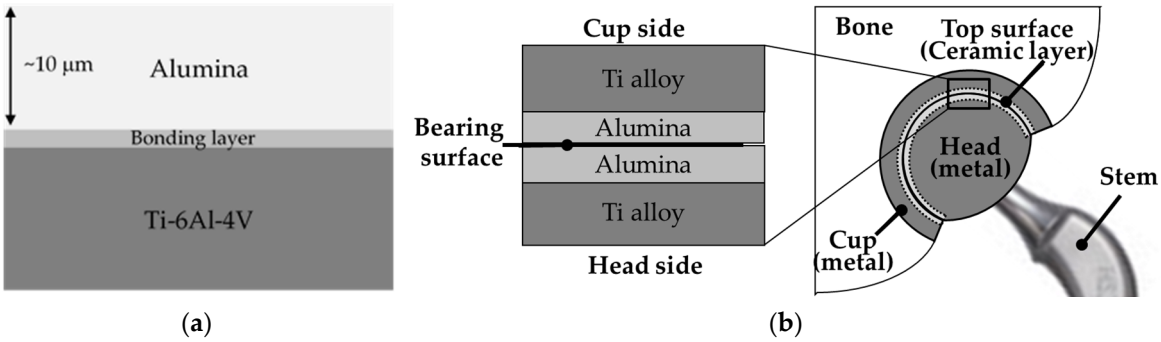

Figure 1. Cross-sectional views of alumina/Ti alloy (ATH) hybrid model (**a**), and ATH-on-ATH configuration of the artificial hip joint (**b**). Reproduced from [102] with permission from Elsevier.

8.2. Rationale for New Artificial Hip Joint Design

Advanced implant designs are focused on reducing wear of bearing surfaces by increasing diameter of heads. Despite being successful in this regard, all MoM, MoP, CoC couples share common issues of edge loading or impingement of taper joint of the stem with the rim of the cup, both of which

result in the release of a large amount of wear debris and thereby leading to high revision rates. Edge loading of the cup is reported in case contact patch between ball and cup extends to the rim of the cup, resulting in an increase in local stresses and more wear at the rim. It could also be the loss of lubrication due to lack of synovial fluid between contacting surfaces [104]. Almost 70% of the MoP implants have been reported to be associated with impingement related rim damage [105]. For CoC implants, incidences of wear of rim have been reported to enhance third body wear, leading to catastrophic fracture of the ceramic part [106]. Evidence of metal wear debris has been reported for both MoM and CoC implant designs, which indicates the wear of taper joint and neck-cup impingement [107,108]. To overcome the major issue of wear of taper joint, an alternative design is proposed in which a single part for both stem and head could be made of the Ti alloy, as shown in Figure 2a. The head portion of Ti alloy could be selectively covered with alumina layer, as shown schematically in Figure 2b. The stemcan be directly bonded to the bone after its porous part of Ti metal is subjected to alkali-heat treatment, as demonstrated by our previous research groups [13,15,109]. This surface treatment technology is currently marketed as AHFIX® by KYOCERA Medical. Clinical reports have demonstrated 98% success rate after ten years of implantation [109].

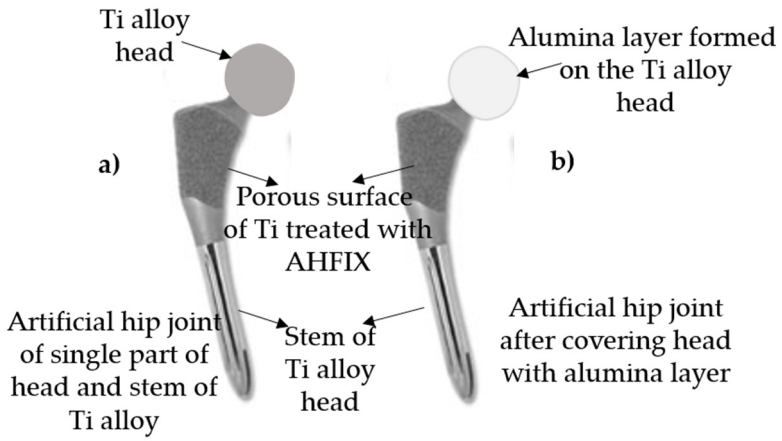

Figure 2. New design of artificial hip joint made of single part of head and stem of Ti alloy before (**a**) and after alumina layer formed on the head part (**b**).

8.3. Science and Technology of Novel Artificial Hip Joint: A Layer of Dense α-Alumina on the Ti Alloy

Conventionally, an alumina layer is fabricated on the metal substrates by plasma spraying of pure α-alumina powders. However, γ-alumina is mostly detected in plasma-sprayed alumina coatings with porous microstructures, leading to poor hardness of 1000–1200 HV, which makes them unsuitable for wear resistance applications. Although anodic oxidation of Al metal [110] or thermal treatments of Al metal layer on Ti alloy [100] have also been attempted to produce α-alumina, a dense and pure α-alumina layer cannot be fabricated using these methods. One of the promising processing strategy to form alumina layer on the Ti alloy includes the deposition of dense Al metal layer onto the Ti alloy and subsequent oxidation of Al.

8.3.1. Formation of Al Layer on the Ti Alloy

In order to form 5–10 μm thick dense α-alumina layers, at least a couple of microns thick layer of Al metal is needed to form on the Ti alloy, which is not yet possible with conventional Al deposition techniques such as PVD [111], arc ion plating [112], and sputtering [113]. Ideally, a method of formation of a thick layer of Al on the Ti alloy substrate should be chosen with minimal or no chemical reaction with the substrate during Al layer formation, which otherwise might lead to formation of thick layer of AlTi intermetallic compounds containing several cracks or pores [114] and leading to delamination of Al layer. To address these needs, cold spraying (CS) technique is used to deposit thick layers of Al

metal on soft metals such as Al alloys [115,116] at temperature much lower than the melting point of Al (T_m = 660 °C). CS technique allows the deposition of a thick metal coating on a metallic substrate by accelerating small particles (<50 μm) to high velocities (500–1500 m/san) by a supersonic jet of compressed gas at a temperature below the melting point of the material to be deposited. In the field of biomaterials, for the first time, dense and thick layers of pure Al with thickness from 250 to 1000 μm were formed on Ti-6Al-4V alloy by CS of Al particles in N_2 or He gas atmosphere at varying pressures of 1–3 MPa and at a temperature of 380 °C [100].

Cold sprayed Al layers (CS-Al) on the Ti alloy formed dense microstructures both in He or N_2 gas atmosphere at an optimal pressure of 3 MPa and a temperature of 380 °C. However, CS-Al layers formed in He atmosphere shows larger cracks or gaps at the interface as a result of higher critical velocities of Al particles (972.5 m/s) [100]. CS-Al layers formed in N_2 gas atmosphere also showed poor adhesion as shown by gaps at the interface as shown in Figure 3a. Nevertheless, these samples showed relatively better adhesion than those treated in He atmosphere which could be due to lower critical velocity of 552.1 m/s in N_2 gas atmosphere. These kinds of gaps could arise due to significant difference in materials properties of Al and Ti alloy or massive plastic deformation within CS-Al layer that might have been caused by ballistic impacts during CS, thereby resulting in accumulation of residual stresses at the interface and ultimately leading to cracks at the interface [101].

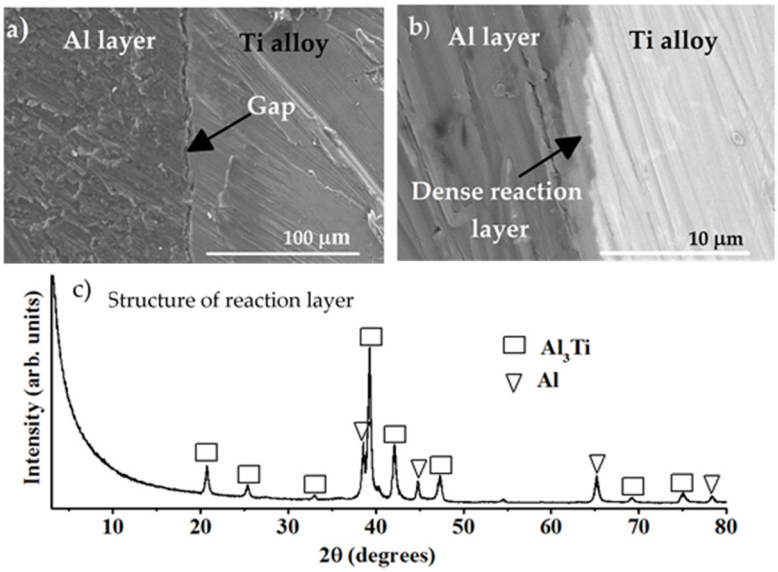

Figure 3. SEM image of Al layer formed on the Ti alloy (**a**), BSE image after heat treatment (**b**), and TF-XRD of the reaction layer (**c**). Reproduced [101] from with permission from Elsevier

8.3.2. Formation of Reaction Layer at Alumina-Ti Alloy Interface

The formation of a reaction layer of AlTi type of intermetallic compound at the interface between CS-Al layer and the Ti alloy substrate could be a promising solution to improve the adhesion and minimize the residual stresses at their interface. In this regard, a heat treatment of CS-Al layer/Ti alloy at 640 °C for 1 h in air or Ar gas atmosphere formed a dense and crack-free reaction layer 2 μm thick at the interface as shown in backscattered electron image (BSE), Figure 3b. This reaction layer could be formed by solid state diffusion of Al into Ti, according to Equation (1), since Al has lower melting point (T_m = 660 °C) as compared with the Ti alloy.

$$Ti\ (s) + 3\ Al\ (s) \rightarrow Al_3Ti\ (s) \quad (1)$$

Thin film XRD (TF-XRD) revealed that the reaction layer is composed of an Al_3Ti intermetallic compound, as shown in Figure 3c. When CS-Al/Ti is heated at 640 °C for more than 3 h or at

temperatures more than 850 °C, a several tens of micrometers thick reaction layer containing a mixture of the AlTi type of intermetallic compounds with several pores or cracks is formed due to differences in densities of thick Ti–Al layer and compacted CS-Al from which it is formed. As a result, thick reaction layers are not be suitable for a load bearing application of artificial hip.

Even though the reaction layer of Al_3Ti layer improves adhesion between Al and Ti, Al_3Ti is itself a brittle intermetallic compound and might be prone to fracture. To reveal the mechanical reliability of Al_3Ti reaction layers, high mechanical load of 500 N was applied by compressing steel balls of 3 mm diameter directly onto the surface of reaction layers. Several large cracks along the periphery of spherical indentation on the thick reaction layer in the SEM image, Figure 4a, suggests a typical signature of brittle fracture which indicate poor mechanical deformability of thick layer, almost like a bulk ceramic. The thin reaction layer of Al_3Ti on the Ti alloy did not reveal any cracks in the SEM image, Figure 4b, suggesting its good mechanical deformability. Sharp Vickers indentations also showed better mechanical reliability of thin reaction layer [101]. Overall, about 2 µm thick reaction layer seems to provide a good interface between alumina and the Ti alloy hybrid.

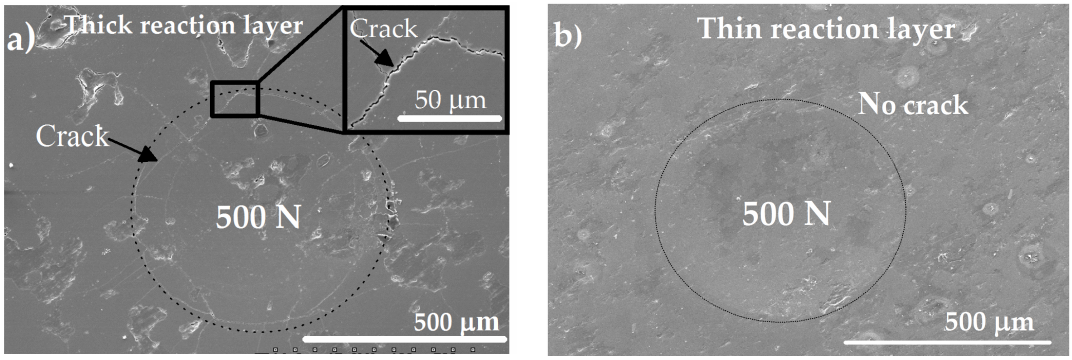

Figure 4. SEM images showing the impressions of ball indentations on the surface of thick after applying a load of 500 N (**a**), and thin reaction layers after applying a load of 500 N (**b**). Reproduced from [101] with permission from Elsevier.

8.3.3. Formation of Alumina Layer on the Ti Alloy

Heat treatment of Al-coated Ti alloy at or above melting point of Al, could result in uncontrolled melting of Al and diffusing into Ti to form an undesirable thick layer of AlTi type of intermetallics along with only small scales of transition alumina. Dense α-alumina starts forming at temperatures above 1000 °C. However, such high temperatures cannot be applied to Al coated onto Ti-6A-4V alloy since an $\alpha \rightarrow \beta$ Ti transformation at 995 °C results in a decrease in the mechanical strength of the alloy, which defeats the purpose of using high strength Ti alloy for the designed hybrid. Attempts were made to form alumina in two steps: firstly by forming a thick layer of Al_3Ti by heating it at 640 °C for 12 h in air and subsequent heat treatment at 850 °C for 96 h [100] according to the Equation (2).

$$2TiAl_3\ (s) + 3/2\ O_2\ (g) \rightarrow 2TiAl_2\ (s) + Al_2O_3\ (s) \quad (2)$$

Thin film XRD revealed that mainly Al_3Ti phase is detected after first heat treatment in Figure 5a and mainly, Al_2Ti phase is detected after subsequent heat treatment in Figure 5b.

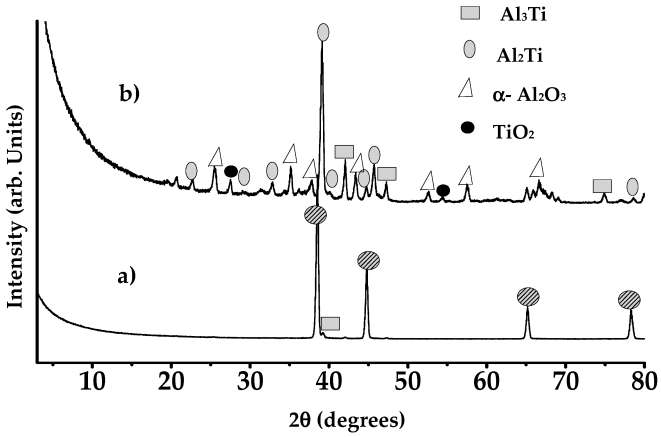

Figure 5. TF-XRD of Al layer on the Ti alloy after heat treatment at 640 °C for 12 h (**a**) and subsequent heat treatment at 850 °C for 96 h (**b**) both in an air atmosphere. Reproduced from [100] with permission from Trans Tech.

Clearly, dense α-alumina cannot be formed on the Ti alloy by using conventional methods such as heat treatments or plasma spraying of alumina. An alternative approach was recently proposed in which CS-Al layer was transformed to a dense alumina layer by micro-arc oxidation (MAO) treatment. MAO is a plasma-assisted electrochemical surface treatment carried out under 400–700 V in a dilute alkaline medium to produce ultra-hard oxide layers on the surface of soft metals such as Al, Mg or Zr for structural applications [117–121]. However, ultra-hard oxide layers formed on the soft metals do not provide the mechanical support for load bearing application of artificial hip joint. Thus, a duplex coating is required to form a α-alumina layer on the Ti alloy. To meet these goals, a promising processing strategy was proposed and demonstrated in which a dense CS-Al layer was formed onto the Ti alloy by cold spraying, followed by heat treatment at 640 °C for 1 h in air to form about 2 μm thick reaction layer to improve adhesion and finally, an optimal MAO treatment of the CS-Al layer to transform it into alumina layer, as shown schematically in Figure 6.

Figure 6. Schematic of deposition of Al layer, followed by heat treatment to form a thin reaction layer at the interface and micro-arc oxidation (MAO) to form alumina.

Compared with MAO treatments of Al in unipolar DC mode, bipolar pulse power supply with electrical parameters of pulse frequency, duty cycle and current density offer control over the electrochemical processes in MAO treatment. Despite many studies performed so far on MAO of Al [117–121], it is not revealed whether a α-alumina layer of at least 10 microns with dense microstructures and high Vickers hardness can be formed. In a quest to reveal this, effects of MAO electrical parameters on phase, purity, thickness and hardness of oxide layers formed by MAO of CS-Al layers/Ti alloy were systematically studied recently to determine the optimal process to form at least 10–20 μm thick layer of pure α-alumina with high Vickers hardness [101,102].

Typically, micro-arc oxidation treatment of Al layer forms a phase and density gradient oxide layer in which outer porous region is composed of mainly γ-alumina and with increasing depth, a mixed α and γ-alumina denser regions are formed in which amount of γ-alumina decreases and that of α-alumina increases and an innermost dense regions containing pure α-alumina is formed as

shown schematically in Figure 7a. Corresponding cross-sectional BSE image of oxide layer formed by MAO of CS-Al/Ti after treatment time of 60 min is shown in Figure 7b. Due to poor thermal conductivity, alumina absorbs heat input to undergo phase transition and as a result, innermost region absorbs maximum heat input to transform to pure α-alumina. Outer surface regions contains mainly γ-alumina and several pores and cracks due to entrapped Si-oxides. Outer surface in contact with electrolytic solution remains relatively cooler than inner regions and hence, does not absorb sufficient heat from discharges [117–121]. As a result, mainly γ-alumina is detected on the outer surface in MAO coatings, as shown in TF-XRD of outer regions of oxide layers in Figure 7c,d. Typically, thin oxide layers (30–40 μm thick) contain γ-alumina as the major phase, which may be due to lack of sufficient heat input to undergo phase transition from $\gamma \rightarrow \alpha$ alumina. Thick oxide layers 90–100 μm or more, absorbs more heat input from intense discharges, which is sufficient to trigger $\gamma \rightarrow \alpha$ alumina phase transition. Outer regions of oxide layer contains several large sized pores and cracks and contain a mixture of α and γ-alumina, which are undesirable due to inferior load bearing support for artificial hip joint application. Moreover, commercial alumina of femoral head is composed of α-alumina phase and has shown long-term *in vivo* stability. From application point of view, the outer regions of oxide layer need to be carefully abraded to reveal an underlying dense α-alumina as shown by TF-XRD of abraded oxide layer in Figure 7e. Subsequent microscopic observations revealed 30 μm α-alumina formed by MAO treatment of Al layer for 60 min [101].

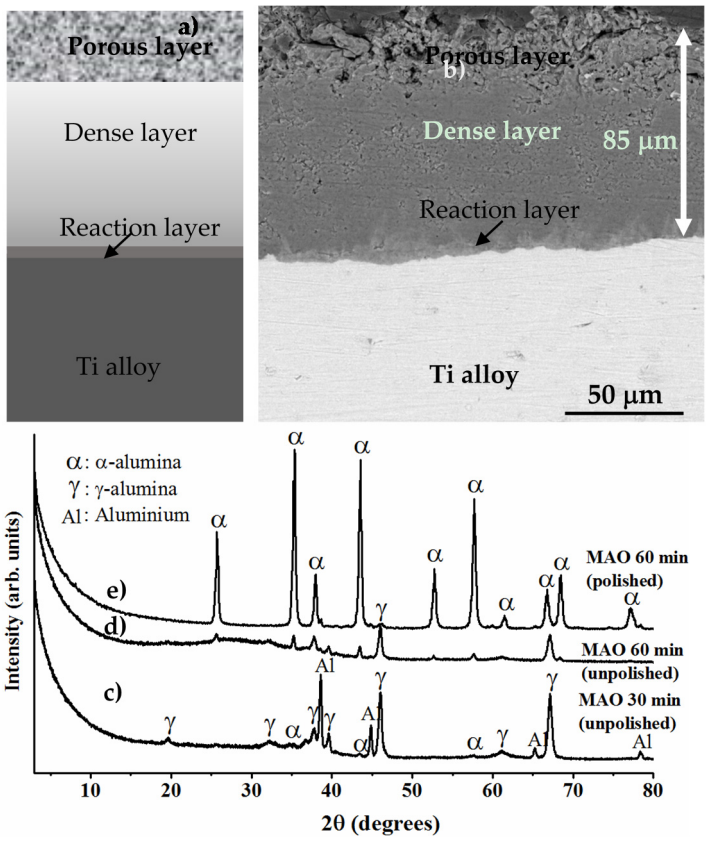

Figure 7. Schematic view of section of designed alumina/Ti alloy model (**a**); corresponding BSE image of alumina layer on the Ti alloy (**b**); and TF-XRDs of CS-Al layer after MAO for 30 min (**c**); 60 min (**d**); and after polishing (**e**). Reproduced from [101] with permission from Elsevier.

Close microscopic observations revealed several small micro-cracks formed within the 30 μm thick, pure α-alumina layer as shown in Figure 8a, which showed Vickers hardness of about 1700 HV; this value is closer to that of commercial alumina but still needs improvement. To increase the hardness

of α-alumina, application of higher frequency in bipolar pulse mode is commonly known to increase thickness of oxide layer which could form a thicker α-alumina layer. These hypotheses were recently corroborated by revealing that thickness of α-alumina layer increased from 30 to 45 µm by increasing pulse frequency from 500 to 1000 Hz, both at a duty cycle of 40%. However, with increasing frequency from 500 to 1000 Hz, mean Vickers hardness decreased from 1658 to 1520 HV since the mean size of micro-cracks increased from 2 to 3 µm [102], as shown in Figure 8b.

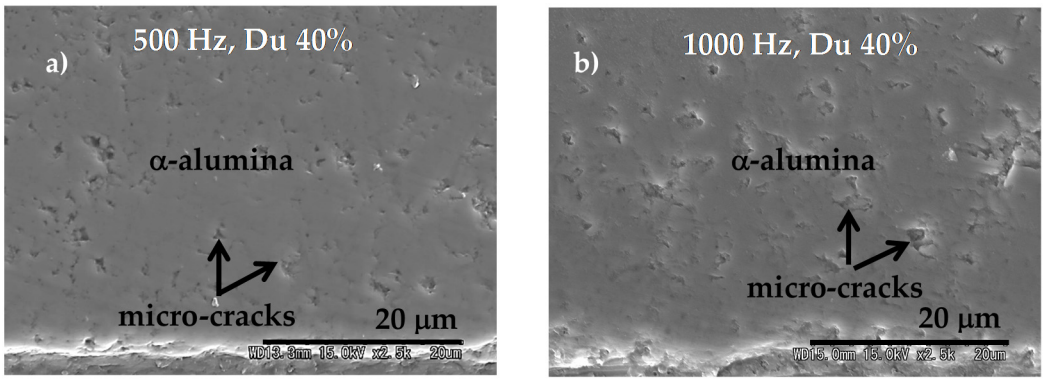

Figure 8. SEM image of cross-section of alumina layer on the Ti alloy formed by MAO of CS-Al layer at pulse frequency of 500 Hz (**a**) and 1000 Hz (**b**) both at duty cycle of 40% for 60 min. Reproduced from [102] with permission from Elsevier.

Another possible way to improve the Vickers hardness of α-alumina is to increase the duty cycle process parameter of MAO treatment. Increasing the duty cycle results in longer working time in a single pulse that imparts large discharge energy within a pulse that might improve sinterability of alumina. It was revealed that increasing duty cycle from 40% to 60% increased Vickers hardness of α-alumina layer from 1658 to 1900 HV, which was reported to be due to decrease in mean micro-crack size from 2 to 1 µm, while the amount or thickness of the layer remained the same [102]. Pure and dense α-alumina formed under optimal MAO parameters of pulse frequency 500 Hz, duty cycle 60% and treatment time of 60 min is typically shown in SEM cross-sectional image (Figure 9).

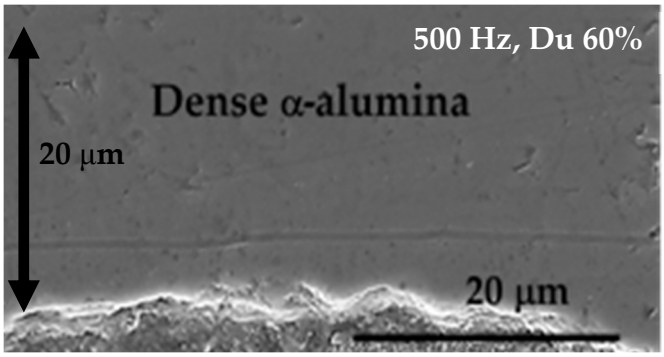

Figure 9. SEM image of cross-section of alumina layer on the Ti alloy formed by MAO of CS-Al layer at pulse frequency of 500 Hz and at duty cycle of 60% for 60 min. Reproduced from [102] with permission from [102].

These findings clearly demarcated the key role of micro-cracks in the densification of the α-alumina layer. Micro-cracks are inherent micro-structural feature in MAO coatings and are difficult to eliminate due to thermal/residual stresses that are generated because of differential cooling rates within graded layer of alumina. To obtain pore or crack free α-alumina, post-laser surface treatments can be applied carefully using Nd-YAG laser.

8.3.4. Adhesion of α-Alumina Layer with the Ti Alloy

In order to realize the potential of ATH for wear resistance applications, the α-alumina layer should have good adhesion to the Ti alloy substrate, which could also ensure good reliability of the joint. Ideally, reaction layer of Al_3Ti between CS-Al layer and the Ti alloy should not be oxidized by MAO treatment. Nevertheless, reaction layer was partially oxidized, which increased its thickness from 2 to 5 μm, as shown in BSE image, Figure 10. To evaluate the adhesion of α-alumina layer, Vickers indentations were made directly at the interfaces. No cracks within or around the impression of indentation were revealed in BSE image, Figure 10, which suggests good adhesion between the alumina layer and the Ti alloy. Grazing angle TF-XRD of the polished α-alumina layer revealed that the phase of reaction layer was changed from Al_3Ti to Al_2TiO_5 [102]. Usually, thermal expansion coefficients of oxides are less than metals or intermetallics; hence, the formation of Al_2TiO_5 might improve the adhesion strength of the joint. However, the thickness of oxidized reaction layer is very critical; if reaction layer is too much oxidized to a thickness of 15–20 μm by increasing MAO treatment time, several cracks are formed at the interface, suggesting poor adhesion [102]. Further quantitative measure of adhesion strength is needed to evaluate its potential for artificial joint applications.

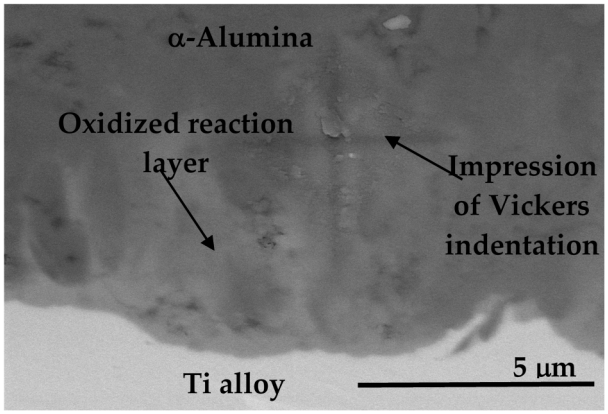

Figure 10. BSE image show sectional view of alumina layer-reaction layer-Ti alloy and impression of Vickers indentation at alumina-Ti interface. Reproduced from [102] with permission from Elsevier.

8.3.5. Dense Alumina Layer on Ti Alloy by Cold Metal Transfer and MAO Methods

Evidently, reaction layer at the interface is needed to improve adhesion between alumina and the Ti alloy, which is generated by heat treatment of cold sprayed Al layer on the Ti alloy [100–102]. If a similar reaction layer at the interface can be formed during Al layer deposition itself, it could eliminate the additional heat treatment step, which could reduce the cost of manufacturing of alumina/Ti alloy hybrids. To explore this possibility, weld cladding method has been commonly used to deposit metal coatings on the substrates using gas metal arc welding (GMAW) or laser cladding. However, composition of deposited metal coating might significantly change due to mixing with the metal substrate during GMAW process, which inadvertently increases the thickness of intermetallics formed at the interface between the coating and the substrate in the case of Al/Fe; similar change might be expected in Al/Ti system, which is undesirable. The thickness of intermetallic reaction layer should be less than 5 μm, which otherwise can result in cracks within the reaction layer due to residual stresses within it.

A promising alternative is to use a low heat input Al deposition method that could result in minimal diffusion of the substrate material into the Al coating to form a thin intermetallic layer. In this regard, cold metal transfer (CMT) method has been shown to form 2–4 μm thick intermetallic layers in joints of Al and Zn-coated steels. CMT method was used for the first time to deposit about 3 mm thick Al layer on the Ti alloy after careful process optimization [103]. Cross-sectional analysis of deposited

layer of Al by CMT method (CMT-Al) revealed 1–1.5 μm thick reaction layer in Figure 11a with gradient compositions indicated by gradual EDS element profiles of Al and Ti in Figure 11b, which suggests formation of AlTi type intermetallic compounds with Al_3Ti as major intermetallic compound, as confirmed by TF-XRD measurements [103]. Optimized MAO process parameters applied to CMT-Al layer on the Ti alloy revealed almost dense α-alumina layer on the Ti alloy as shown in Figure 11c, while retaining the nascent gradient reaction layer at the interface as shown by EDS elemental line profies of Al and Ti in Figure 11d.

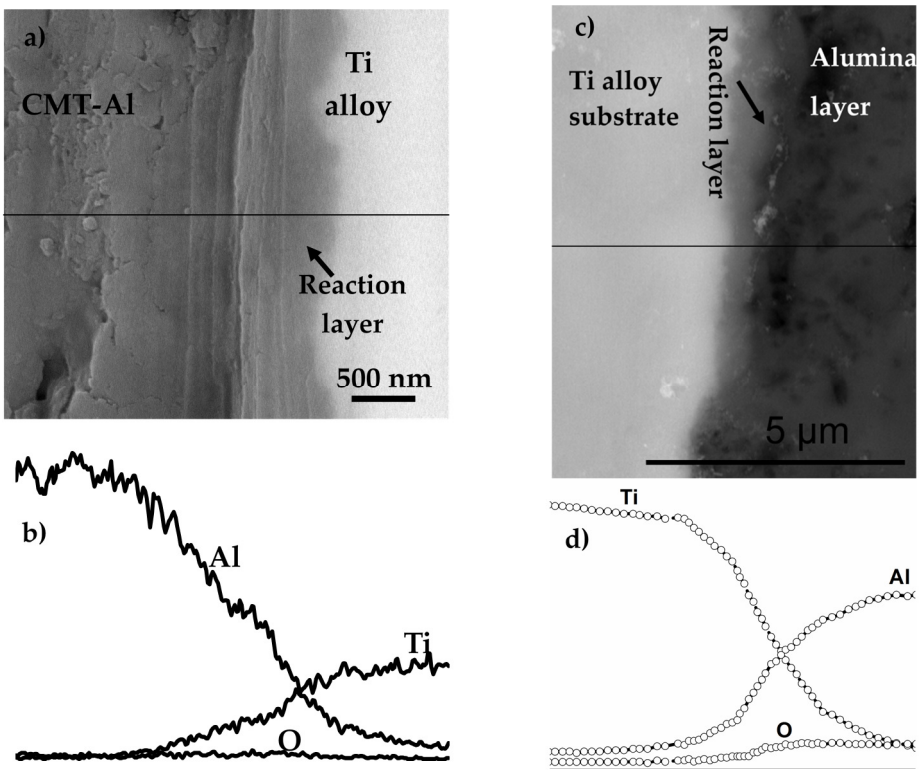

Figure 11. BSE image and line profile of cross-section of CMT-Al: Before MAO treatment (**a**,**b**); and after MAO treatment (**c**,**d**). Reproduced from [103] with permission from Cambridge Core.

This kind of gradient reaction layer could offer better mechanical reliability to the joint between alumina and the Ti alloy by minimizing the residual stresses at their interfaces and avoiding steep changes in physical or mechanical properties from top ceramic layer to the Ti alloy substrate. This is the major issue that has restricted the use of alumina/Ti hybrid combination for applications in many other R&D fields over many decades. Close transmission electron microscopy (TEM) analysis of the structures of this gradient reaction layer is further needed, which could provide the guidelines for designing future generation ceramic-metal hybrid based prosthetic devices with high mechanical reliability.

9. Summary and Conclusions

Comparing to bulk alumina used for the femoral head, studies suggested that dense α-alumina layers with high Vickers hardness and better mechanical reliability can be successfully fabricated onto the Ti alloy using a combination of cold spray or cold metal transfer and micro-arc oxidation methods. A schematic of cross-section of designed alumina/Ti alloy hybrid is shown in Figure 12.

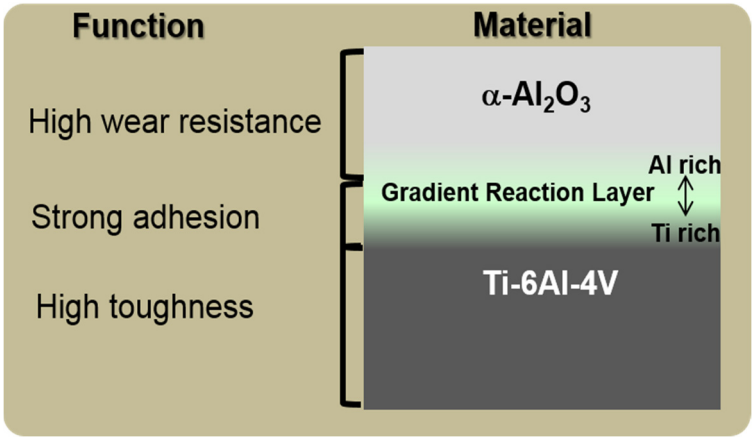

Figure 12. Schematic of cross-sectional view of a α-alumina layer on the Ti alloy with a gradient reaction layer at their interface. Reproduced from [103] with permission from Cambridge Core.

This designed alumina/Ti alloy could be a potential candidate for future generation of artificial hip joint prostheses. These investigations also suggest that the combination of cold spray or cold metal transfer and micro-arc oxidation methods will be effective in forming an adherent layer of dense α-alumina and is expected to enable advances in the field of artificial hip joints. The designed ceramic/metal hybrid technology is novel in a broad sense since it can be suitably applied to other medical implants such as knee joint and as a dense ceramic coating on Ti metal for dental implants. Before considering these hybrids for commercial applications, it is necessary to evaluate the cytotoxicity, inflammatory responses, and chemical analyses of wear debris of alumina layer on the Ti alloy subjected to tribological testing as well as TEM analysis of the interfaces between the alumina layer-reaction layer-Ti alloy and corrosion testing of the reaction layer. The outcomes of these investigations will provide paths forward for the possibility of extending the research methodologies to develop a femoral head of dense α-alumina layer on the Ti alloy.

Conflicts of Interest: The authors declare no conflict of interest.

References

1. Kurtz, S.; Ong, K.; Lau, E.; Mowat, F.; Halpern, M. Projections of primary and revision hip and knee arthroplasty in the United States from 2005 to 2030. *J. Bone Jt. Surg. Am.* **2007**, *89*, 780–785. [CrossRef]
2. Renkawitz, T.; Santori, F.S.; Grifka, J.; Valverde, C.; Morlock, M.M.; Learmonth, I.D. A new short uncemented, proximally fixed anatomic femoral implant with a prominent lateral flare: Design rationals and study design of an international clinical trial. *BMC Musculoskelet. Disord.* **2008**, *9*, 147. [CrossRef] [PubMed]
3. Steens, W.; Boettner, F.; Bader, R.; Skripitz, R.; Schneeberger, A. Bone mineral density after implantation of a femoral neck hip prosthesis-a prospective 5 year follow-up. *BMC Musculoskelet. Disord.* **2015**, *16*, 192. [CrossRef] [PubMed]
4. Miura, K.; Yamada, N.; Hanada, S.; Jung, T.K.; Itoi, E. The bone tissue compatibility of a new Ti-Nb-Sn alloy with a low Young's modulus. *Acta Biomater.* **2011**, *7*, 2320–2326. [CrossRef] [PubMed]
5. Guo, S.; Bao, Z.Z.; Meng, Q.K.; Hu, L.; Zhao, X.Q. A novel metastable Ti-25Nb-2Mo-4Sn alloy with high strength and low Young's modulus. *Metall. Mater. Trans. A Phys. Metall. Mater. Sci.* **2012**, *43*, 3447–3451. [CrossRef]
6. Niinomi, M.; Hattori, T.; Morikawa, K.; Kasuga, T.; Suzuki, A.; Fukui, H.; Niwa, S. Development of low rigidity beta-type titanium alloy for biomedical applications. *Mater. Trans.* **2002**, *43*, 2970–2977. [CrossRef]
7. Okazaki, Y. A new Ti-15Zr-4Nb-4Ta alloy for medical applications. *Curr. Opin. Solid State Mater. Sci.* **2001**, *5*, 45–53. [CrossRef]
8. Bai, X.; Sandukas, S.; Appleford, M.R.; Ong, J.L.; Rabiei, A. Deposition and investigation of functionally graded calcium phosphate coatings on titanium. *Acta Biomater.* **2009**, *5*, 3563–3572. [CrossRef] [PubMed]

9. Bai, X.; Sandukas, S.; Appleford, M.; Ong, J.L.; Rabiei, A. Antibacterial effect and cytotoxicity of Ag-doped functionally graded hydroxyapatite coatings. *J. Biomed. Mater. Res. Part B Appl. Biomater.* **2012**, *100*, 553–561. [CrossRef] [PubMed]
10. Chen, W.; Liu, Y.; Courtney, H.S.; Bettenga, M.; Agrawal, C.M.; Bumgardner, J.D.; Ong, J.L. *In vitro* anti-bacterial and biological properties of magnetron co-sputtered silver-containing hydroxyapatite coating. *Biomaterials* **2006**, *27*, 5512–5517. [CrossRef] [PubMed]
11. Ong, J.L.; Lucas, L.C.; Lacefield, W.R.; Rigney, E.D. Structure solubility and bond strength of thin calcium-phosphate coatings produced by ion-beam sputter deposition. *Biomaterials* **1992**, *13*, 249–254. [CrossRef]
12. Yang, Y.Z.; Kim, K.H.; Ong, J.L. Review on calcium phosphate coatings produced using a sputtering process—an alternative to plasma spraying. *Biomaterials* **2005**, *26*, 327–337. [CrossRef] [PubMed]
13. Kim, H.M.; Miyaji, F.; Kokubo, T.; Nakamura, T. Preparation of bioactive Ti and its alloys via simple chemical surface treatment. *J. Biomed. Mater. Res.* **1996**, *32*, 409–417. [CrossRef]
14. Kim, H.M.; Miyaji, F.; Kokubo, T.; Nishiguchi, S.; Nakamura, T. Graded surface structure of bioactive titanium prepared by chemical treatment. *J. Biomed. Mater. Res.* **1999**, *45*, 100–107. [CrossRef]
15. Kim, H.M.; Takadama, H.; Miyaji, F.; Kokubo, T.; Nishiguchi, S.; Nakamura, T. Formation of bioactive functionally graded structure on Ti-6Al-4V alloy by chemical surface treatment. *J. Mater. Sci. Mater. Med.* **2000**, *11*, 555–559. [CrossRef] [PubMed]
16. Kizuki, T.; Takadama, H.; Matsushita, T.; Nakamura, T.; Kokubo, T. Preparation of bioactive Ti metal surface enriched with calcium ions by chemical treatment. *Acta Biomater.* **2010**, *6*, 2836–2842. [CrossRef] [PubMed]
17. Kokubo, T.; Pattanayak, D.K.; Yamaguchi, S.; Takadama, H.; Matsushita, T.; Kawai, T.; Takemoto, M.; Fujibayashi, S.; Nakamura, T. Positively charged bioactive Ti metal prepared by simple chemical and heat treatments. *J. R. Soc. Interface* **2010**, *7*, S503–S513. [CrossRef] [PubMed]
18. Oral, E.; Christensen, S.D.; Malhi, A.S.; Wannomae, K.K.; Muratoglu, O.K. Wear resistance and mechanical properties of highly cross-linked, ultrahigh-molecular weight polyethylene doped with vitamin E. *J. Arthroplast.* **2006**, *21*, 580–591. [CrossRef] [PubMed]
19. Oral, E.; Muratoglu, O.K. Vitamin E diffused, highly crosslinked UHMWPE: A review. *Int. Orthop.* **2011**, *35*, 215–223. [CrossRef] [PubMed]
20. Moro, T.; Kawaguchi, H.; Ishihara, K.; Kyomoto, M.; Karita, T.; Ito, H.; Nakamura, K.; Takatori, Y. Wear resistance of artificial hip joints with poly(2-methacryloyloxyethyl phosphorylcholine) grafted polyethylene: Comparisons with the effect of polyethylene cross-linking and ceramic femoral heads. *Biomaterials* **2009**, *30*, 2995–3001. [CrossRef] [PubMed]
21. Kyomoto, M.; Moro, T.; Iwasaki, Y.; Miyaji, F.; Kawaguchi, H.; Takatori, Y.; Nakamura, K.; Ishihara, K. Superlubricious surface mimicking articular cartilage by grafting poly(2-methacryloyloxyethyl phosphorylcholine) on orthopaedic metal bearings. *J. Biomed. Mater. Res. Part A* **2009**, *91*, 730–741. [CrossRef] [PubMed]
22. Clarke, I.C.; Manaka, M.; Green, D.D.; Williams, P.; Pezzotti, G.; Kim, Y.H.; Ries, M.; Sugano, N.; Sedel, L.; Delauney, C.; et al. Current status of zirconia used in total hip implants. *J. Bone Jt. Surg. Am.* **2003**, *85*, 73–84. [CrossRef]
23. Begand, S.; Oberbach, T.; Glien, W. Investigations of the mechanical properties of an alumina toughened zirconia ceramic for an application in joint prostheses. *Key Eng. Mater.* **2005**, *284*, 1019–1022. [CrossRef]
24. Al-Hajjar, M.; Jennings, L.M.; Begand, S.; Oberbach, T.; Delfosse, D.; Fisher, J. Wear of novel ceramic-on-ceramic bearings under adverse and clinically relevant hip simulator conditions. *J. Biomed. Mater. Res. Part B Appl. Biomater.* **2013**, *101*, 1456–1462. [CrossRef] [PubMed]
25. Hobbs, L.W.; Rosen, V.B.; Mangin, S.P.; Treska, M.; Hunter, G. Oxidation microstructures and interfaces in the oxidized zirconium knee. *Int. J. Appl. Ceram. Technol.* **2005**, *2*, 221–246. [CrossRef]
26. Good, V.; Ries, M.; Barrack, R.L.; Widding, K.; Hunter, G.; Heuer, D. Reduced wear with oxidized zirconium femoral heads. *J. Bone Jt. Surg. Am.* **2003**, *85*, 105–110. [CrossRef]
27. Burger, W.; Richter, H.G. High strength and toughness alumina matrix composites by transformation toughening and 'in situ' platelet reinforcement (ZPTA)—The new generation of bioceramics. *Key Eng. Mater.* **2000**, *192–195*, 545–548. [CrossRef]
28. Brown, A.S. Hip New World. *ASME Mech. Eng.* **2006**, *128*, 28–33.

29. Charnley, J.; Kamangar, A.; Longfield, M.D. The optimum size of prosthetic heads in relation to wear of plastic sockets in total replacement of hip. *Med. Biol. Eng. Comput.* **1969**, *7*, 31–39. [CrossRef]
30. Amstutz, H.C.; Campbell, P.; Kossovsky, N.; Clarke, I.C. Mechanism and clinical significance of wear debris-induced osteolysis. *Clin. Orthop. Relat. Res.* **1992**, *276*, 7–18. [CrossRef]
31. Boutin, P. Total arthroplasty of the hip by fritted alumina prosthesis. Experimental study and 1st clinical applications. *Orthop. Traumatol. Surg. Res.* **2014**, *100*, 15–21. [CrossRef] [PubMed]
32. Harris, W.H. The prolem is osteolysis. *Clin. Orthop. Relat. Res.* **1995**, *311*, 46–53.
33. Kim, Y.H.; Kim, J.S.; Park, J.W.; Joo, J.H. Periacetabular osteolysis is the problem in contemporary total hip arthroplasty in young patients. *J. Arthroplast.* **2012**, *27*, 74–81. [CrossRef] [PubMed]
34. Kurtz, S. Compendium of highly crosslinked UHMWPEs. In *UHMWPE Biomaterials Handbook*; Kurtz, S., Ed.; Elsevier: New York, NY, USA, 2009; pp. 291–308.
35. Oral, E.; Malhi, A.S.; Muratoglu, O.K. Mechanisms of decrease in fatigue crack propagation resistance in irradiated and melted UHMWPE. *Biomaterials* **2006**, *27*, 917–925. [CrossRef] [PubMed]
36. Reinitz, S.D.; Currier, B.H.; Van Citters, D.W.; Levine, R.A.; Collier, J.P. Oxidation and other property changes of retrieved sequentially annealed UHMWPE acetabular and tibial bearings. *J. Biomed. Mater. Res. Part B Appl. Biomater.* **2015**, *103*, 578–586. [CrossRef] [PubMed]
37. Oral, E.; Neils, A.L.; Doshi, B.N.; Fu, J.; Muratoglu, O.K. Effects of simulated oxidation on the *in vitro* wear and mechanical properties of irradiated and melted highly crosslinked UHMWPE. *J. Biomed. Mater. Res. Part B Appl. Biomater.* **2016**, *104*, 316–322. [CrossRef] [PubMed]
38. Bhateja, S.K.; Duerst, R.W.; Aus, E.B.; Andrews, E.H. Free radicals trapped in polyethylene crystals. *J. Macromol. Sci. Part B Phys.* **1995**, *34*, 263–272. [CrossRef]
39. Jahan, M.S.; King, M.C.; Haggard, W.O.; Sevo, K.L.; Parr, J.E. A study of long-lived free radicals in gamma-irradiated medical grade polyethylene. *Radiat. Phys. Chem.* **2001**, *62*, 141–144. [CrossRef]
40. Lewis, G. Properties of crosslinked ultra-high-molecular-weight polyethylene. *Biomaterials* **2001**, *22*, 371–401. [CrossRef]
41. Dumbleton, J.H.; D'Antonio, J.A.; Manley, M.T.; Capello, W.N.; Wang, A. The basis for a second-generation highly cross-linked UHMWPE. *Clin. Orthop. Relat. Res.* **2006**, *453*, 265–271. [CrossRef] [PubMed]
42. Currier, B.H.; Van Citters, D.W.; Currier, J.H.; Carlson, E.M.; Tibbo, M.E.; Collier, J.P. *In vivo* oxidation in retrieved highly crosslinked tibial inserts. *J. Biomed. Mater. Res. Part B Appl. Biomater.* **2013**, *101*, 441–448. [PubMed]
43. Kurtz, S.M.; Gawel, H.A.; Patel, J.D. History and systematic review of wear and osteolysis outcomes for first-generation highly crosslinked polyethylene. *Clin. Orthop. Relat. Res.* **2011**, *469*, 2262–2277. [CrossRef] [PubMed]
44. Oral, E.; Neils, A.L.; Wannomae, K.K.; Muratoglu, O.K. Novel active stabilization technology in highly crosslinked UHMWPEs for superior stability. *Radiat. Phys. Chem.* **2014**, *105*, 6–11. [CrossRef]
45. Green, J.M.; Hallab, N.J.; Liao, Y.S.; Narayan, V.; Schwarz, E.M.; Xie, C. Anti-oxidation treatment of ultra high molecular weight polyethylene components to decrease periprosthetic osteolysis: Evaluation of osteolytic and osteogenic properties of wear debris particles in a murine calvaria model. *Curr. Rheumatol. Rep.* **2013**, *15*, 325. [CrossRef] [PubMed]
46. Sillesen, N.H.; Greene, M.E.; Nebergall, A.K.; Nielsen, P.T.; Laursen, M.B.; Troelsen, A.; Malchau, H. Three year RSA evaluation of vitamin E diffused highly cross-linked polyethylene liners and cup stability. *J. Arthroplast.* **2015**, *30*, 1260–1264. [CrossRef] [PubMed]
47. Ishihara, K. Highly lubricated polymer interfaces for advanced artificial hip joints through biomimetic design. *Polym. J.* **2015**, *47*, 585–597. [CrossRef]
48. Bragdon, C.R.; Doerner, M.; Martell, J.; Jarrett, B.; Palm, H.; Malchau, H. The 2012 John Charnley Award: Clinical multicenter studies of the wear performance of highly crosslinked remelted polyethylene in THA. *Clin. Orthop. Relat. Res.* **2013**, *471*, 393–402. [CrossRef] [PubMed]
49. Skipor, A.K.; Campbell, P.A.; Patterson, L.M.; Anstutz, H.C.; Schmalzried, T.P.; Jacobs, J.J. Serum and urine metal levels in patients with metal-on-metal surface arthroplasty. *J. Mater. Sci. Mater. Med.* **2002**, *13*, 1227–1234. [CrossRef] [PubMed]
50. Catelas, I.; Wimmer, M.A. New insights into wear and biological effects of metal-on-metal bearings. *J. Bone Jt. Surg. Am.* **2011**, *93*, 76–83. [CrossRef] [PubMed]

51. Basketter, D.A.; Briaticovangosa, G.; Kaestner, W.; Lally, C.; Bontinck, W.J. Nickel, cobalt and chromium in consumer products: A role in allergic contact-dermatitis? *Contact Dermat.* **1993**, *28*, 15–25. [CrossRef]
52. Head, W.C.; Bauk, D.J.; Emerson, R.H. Titanium as the material of choice for cementless femoral components in total hip arthroplasty. *Clin. Orthop. Relat. Res.* **1995**, *311*, 85–90.
53. Walker, P.R.; Leblanc, J.; Sikorska, M. Effects of aluminum and other cations on the structure of brain and liver chromatin. *Biochemistry* **1989**, *28*, 3911–3915. [CrossRef] [PubMed]
54. Rao, S.; Ushida, T.; Tateishi, T.; Okazaki, Y.; Asao, S. Effect of Ti, Al, and V ions on the relative growth rate of fibroblasts (L929) and osteoblasts (MC3T3-E1) cells. *Bio-Med. Mater. Eng.* **1996**, *6*, 79–86.
55. Long, M.; Crooks, R.; Rack, H.J. High-cycle fatigue performance of solution-treated metastable-beta titanium alloys. *Acta Mater.* **1999**, *47*, 661–669. [CrossRef]
56. Guleryuz, H.; Cimenoglu, H. Surface modification of a Ti-6Al-4V alloy by thermal oxidation. *Surf. Coat. Technol.* **2005**, *192*, 164–170. [CrossRef]
57. Guleryuz, H.; Cimenoglu, H. Effect of thermal oxidation on corrosion and corrosion-wear behaviour of a Ti–6Al–4V alloy. *Biomaterials* **2004**, *25*, 3325–3333. [CrossRef] [PubMed]
58. Singh, R.; Kurella, A.; Dahotre, N.B. Laser surface modification of Ti–6Al–4V: Wear and corrosion characterization in simulated biofluid. *J. Biomater Appl.* **2006**, *21*, 49–73. [CrossRef] [PubMed]
59. Li, B.; Shen, Y.; Hu, W.; Luo, L. Surface modification of Ti-6Al-4V alloy via friction-stir processing: Microstructure evolution and dry sliding wear performance. *Surf. Coat. Technol.* **2014**, *239*, 160–170. [CrossRef]
60. Oonishi, H.; Clarke, I.C.; Good, V.; Amino, H.; Ueno, M.; Masuda, S.; Oomamiuda, K.; Ishimaru, H.; Yamamoto, M.; Tsuji, E. Needs of bioceramics to longevity of total joint arthroplasty. *Key Eng. Mater.* **2003**, *240–242*, 735–754. [CrossRef]
61. Sedel, L. Evolution of alumina-on-alumina implants—A review. *Clin. Orthop. Relat. Res.* **2000**, *379*, 48–54. [CrossRef]
62. Sedel, L. Clinical applications of ceramic-ceramic combinations in joint replacement. In *Bioceramics and Their Clinical Applications*; Kokubo, T., Ed.; Woohhead: Cambridge, UK; CRC: Boca Raton, FL, USA, 2008; pp. 688–698.
63. Jarrett, C.A.; Ranawat, A.S.; Bruzzone, M.; Blum, Y.C.; Rodriguez, J.A.; Ranawat, C.S. The squeaking hip: a phenomenon of ceramic-on-ceramic total hip arthroplasty. *J. Bone Jt. Surg. Am.* **2009**, *91*, 1344–1349. [CrossRef] [PubMed]
64. Hannouche, D.; Zaoui, A.; Zadegan, F.; Sedel, L.; Nizard, R. Thirty years of experience with alumina-on-alumina bearings in total hip arthroplasty. *Int. Orthop.* **2011**, *35*, 207–213. [CrossRef] [PubMed]
65. Clarke, I.C.; Manley, M.T. How do alternative bearing surfaces influence wear behavior? *J. Am. Acad. Orthop. Surg.* **2008**, *16*, S86–S93. [CrossRef] [PubMed]
66. Tipper, J.L.; Hatton, A.; Nevelos, J.E.; Ingham, E.; Doyle, C.; Streicher, R.; Nevelos, A.B.; Fisher, J. Alumina-alumina artificial hip joints. Part II: Characterisation of the wear debris from *in vitro* hip joint simulations. *Biomaterials* **2002**, *23*, 3441–3448. [CrossRef]
67. Bizot, P.; Banallec, L.; Sedel, L.; Nizard, R. Alumina-on-alumina total hip prostheses in patients 40 years of age or younger. *Clin. Orthop. Relat. Res.* **2000**, *379*, 68–76. [CrossRef]
68. Bizot, P.; Larrouy, M.; Witvoet, J.; Sedel, L.; Nizard, R. Press-fit metal-backed alumina sockets: A minimum 5-year followup study. *Clin. Orthop. Relat. Res.* **2000**, *379*, 134–142. [CrossRef]
69. Kim, Y.H.; Kim, J.S.; Cho, S.H. A comparison of polyethylene wear in hips with cobalt-chrome or zirconia heads. A prospective, randomised study. *J. Bone Jt. Surg. Br.* **2001**, *83*, 742–750. [CrossRef]
70. Wroblewski, M.; Siney, P.D.; Nagai, H.; Fleming, P.A. Wear of ultra-high-molecular-weight polyethylene cup articulating with 22.225 mm zirconia diameter head in cemented total hip arthroplasty. *J. Orthop. Sci.* **2004**, *9*, 253–255. [CrossRef] [PubMed]
71. Skyrme, A.D.; Richards, S.; John, A.; Chia, M.; Walter, W.K.; Walter, W.L.; Zicat, B. Polyethylene wear rates with Zirconia and cobalt chrome heads in the ABG hip. *Hip Int.* **2005**, *15*, 63–70. [CrossRef] [PubMed]
72. Piconi, C.; Maccauro, G.; Pilloni, L.; Burger, W.; Muratori, F.; Richter, H.G. On the fracture of a zirconia ball head. *J. Mater. Sci. Mater. Med.* **2006**, *17*, 289–300. [CrossRef] [PubMed]
73. Kurtz, S.M.; Kocagoz, S.; Arnholt, C.; Huet, R.; Ueno, M.; Walter, W.L. Advances in zirconia toughened alumina biomaterials for total joint replacement. *J. Mech. Behav. Biomed. Mater.* **2014**, *31*, 107–116. [CrossRef] [PubMed]

74. Green, D.; Pezzotti, G.; Sakakura, S.; Ries, M.; Clarke, I. Zirconia ceramic femoral heads in the USA-retrieved zirconia heads-2 to 10 years out. In Proceedings of the 49th Annual Meeting of the Orthopaedic Research Society, New Orleans, LA, USA, 2–5 February 2003.
75. Bal, B.S.; Rahaman, M.N. Orthopedic applications of silicon nitride ceramics. *Acta Biomater.* **2012**, *8*, 2889–2898. [CrossRef] [PubMed]
76. McEntire, B.J.; Bal, B.S.; Rahaman, M.N.; Chevalier, J.; Pezzotti, G. Ceramics and ceramic coatings in orthopaedics. *J. Eur. Ceram. Soc.* **2015**, *35*, 4327–4369. [CrossRef]
77. Chen, F.C.; Ardell, A.J. Fracture toughness of ceramics and semi-brittle alloys using a miniaturized disk-bend test. *Mater. Res. Innov.* **2000**, *3*, 250–262. [CrossRef]
78. Roebben, G.; Sarbu, C.; Lube, T.; Van der Biest, O. Quantitative determination of the volume fraction of intergranular amorphous phase in sintered silicon nitride. *Mater. Sci. Eng. A* **2004**, *370*, 453–458. [CrossRef]
79. Olofsson, J.; Pettersson, M.; Teuscher, N.; Heilmann, A.; Larsson, K.; Grandfield, K.; Persson, C.; Jacobson, S.; Engqvist, H. Fabrication and evaluation of Si*x*N*y* coatings for total joint replacements. *J. Mater. Sci. Mater. Med.* **2012**, *23*, 1879–1889. [CrossRef] [PubMed]
80. Pettersson, M.; Berlind, T.; Schmidt, S.; Jacobson, S.; Hultman, L.; Persson, C.; Engqvist, H. Structure and composition of silicon nitride and silicon carbon nitride coatings for joint replacements. *Surf. Coat. Technol.* **2013**, *235*, 827–834. [CrossRef]
81. Bal, B.S.; Khandkar, A.; Lakshminarayanan, R.; Clarke, I.; Hoffman, A.A.; Rahaman, M.N. Fabrication and testing of silicon nitride bearings in total hip arthroplasty winner of the 2007 "HAP" PAUL Award. *J. Arthroplast.* **2009**, *24*, 110–116. [CrossRef] [PubMed]
82. McEntire, B.J.; Lakshminarayanan, R.; Ray, D.A.; Clarke, I.C.; Puppulin, L.; Pezzotti, G. Silicon nitride bearings for total joint arthroplasty. *Lubricants* **2016**, *4*, 35. [CrossRef]
83. Green, D.; Donaldson, T.; Williams, P.; Pezzotti, G.; Clarke, I. Long term strip wear rates of 3rd and 4th generation ceramic-on-ceramic under microseparation. In Proceedings of the 53rd Annual Meeting of the Orthopaedic Research Society, San Diego, CA, USA, 11–14 February 2007; p. 1776.
84. Clarke, I.; Gustafson, A. The design of ceramics for joint replacement. In *Bioceramics and Their Clinical Applications*; Kokubo, T., Ed.; Woodhead: Cambridge, UK, 2008; pp. 106–132.
85. Begand, S.; Oberbach, T.; Glien, W. ATZ—A new material with a high potential in joint replacement. *Key Eng. Mater.* **2005**, *284–286*, 983–986. [CrossRef]
86. Kremers, H.M.; Larson, D.R.; Crowson, C.S.; Kremers, W.K.; Washington, R.E.; Steiner, C.A.; Jiranek, W.A.; Berry, D.J. Prevalence of total hip and knee replacement in the United States. *J. Bone Jt. Surg. Am.* **2015**, *97*, 1386–1397. [CrossRef] [PubMed]
87. Abu-Amer, Y.; Darwech, I.; Clohisy, J.C. Aseptic loosening of total joint replacements: Mechanisms underlying osteolysis and potential therapies. *Arthritis Res. Ther.* **2007**, *9*, S6. [CrossRef] [PubMed]
88. Narayan, R.J. Nanostructured diamondlike carbon thin films for medical applications. *Mater. Sci. Eng. C* **2005**, *25*, 405–416. [CrossRef]
89. Pappas, M.J.; Makris, G.; Buechel, F.F. Titanium nitride ceramic film against polyethylene: A 48-million cycle wear test. *Clin. Orthop. Relat. Res.* **1995**, *317*, 64–70.
90. Hauert, R.; Falub, C.V.; Thorwarth, G.; Thorwarth, K.; Affolter, C.; Stiefel, M.; Podleska, L.E.; Taeger, G. Retrospective lifetime estimation of failed and explanted diamond-like carbon coated hip joint balls. *Acta Biomater.* **2012**, *8*, 3170–3176. [CrossRef] [PubMed]
91. Choudhury, D.; Lackner, J.M.; Major, L.; Morita, T.; Sawae, Y.; Bin Mamat, A.; Stavness, I.; Roy, C.K.; Krupka, I. Improved wear resistance of functional diamond like carbon coated Ti-6Al-4V alloys in an edge loading conditions. *J. Mech. Behav. Biomed. Mater.* **2016**, *59*, 586–595. [CrossRef] [PubMed]
92. Catledge, S.A.; Vohra, Y.K. Effect of nitrogen addition on the microstructure and mechanical properties of diamond films grown using high-methane concentrations. *J. Appl. Phys.* **1999**, *86*, 698–700. [CrossRef]
93. Catledge, S.A.; Vaid, R.; Diggins, P.; Weimer, J.J.; Koopman, M.; Vohra, Y.K. Improved adhesion of ultra-hard carbon films on cobalt-chromium orthopaedic implant alloy. *J. Mater. Sci. Mater. Med.* **2011**, *22*, 307–316. [CrossRef] [PubMed]
94. Papo, M.J.; Catledge, S.A.; Vohra, Y.K. Mechanical wear behavior of nanocrystalline and multilayer diamond coatings on temporomandibular joint implants. *J. Mater. Sci. Mater. Med.* **2004**, *15*, 773–777. [CrossRef] [PubMed]

95. Amaral, M.; Abreu, C.S.; Oliveira, F.J.; Gomes, J.R.; Silva, R.F. Tribological characterization of NCD in physiological fluids. *Diam. Relat. Mater.* **2008**, *17*, 848–852. [CrossRef]
96. Vila, M.; Amaral, M.; Oliveira, F.J.; Silva, R.F.; Fernandes, A.J.S.; Soares, M.R. Residual stress minimum in nanocrystalline diamond films. *Appl. Phys. Lett.* **2006**, *89*, 093109. [CrossRef]
97. Ries, M.D.; Salehi, A.; Widding, K.; Hunter, G. Polyethylene wear performance of oxidized zirconium and cobalt-chromium knee components under abrasive conditions. *J. Bone Jt. Surg. Am.* **2002**, *84*, 129–135. [CrossRef]
98. Evangelista, G.T.; Fulkerson, E.; Kummer, E.; Di Cesare, P.E. Surface damage to an Oxinium femoral head prosthesis after dislocation. *J. Bone Jt. Surg. Br.* **2007**, *89*, 535–537. [CrossRef] [PubMed]
99. Jaffe, W.L.; Strauss, E.J.; Cardinale, M.; Herrera, L.; Kummer, F.J. Surface oxidized zirconium total hip arthroplasty head damage due to closed reduction. *J. Arthroplast.* **2009**, *24*, 898–902. [CrossRef] [PubMed]
100. Khanna, R.; Matsushita, T.; Kokubo, T.; Takadama, H. Formation of alumina layer on Ti alloy for artificial hip joint. *Key Eng. Mater.* **2014**, *614*, 200–205. [CrossRef]
101. Khanna, R.; Kokubo, T.; Matsushita, T.; Nomura, Y.; Nose, N.; Oomori, Y.; Yoshida, T.; Wakita, K.; Takadama, H. Novel artificial hip joint: A layer of alumina on Ti–6Al–4V alloy formed by micro-arc oxidation. *Mater. Sci. Eng. C* **2015**, *55*, 393–400. [CrossRef] [PubMed]
102. Khanna, R.; Kokubo, T.; Matsushita, T.; Takadama, H. Fabrication of dense α-alumina layer on Ti–6Al–4V alloy hybrid for bearing surfaces of artificial hip joint. *Mater. Sci. Eng. C* **2016**, *69*, 1229–1239. [CrossRef] [PubMed]
103. Khanna, R.; Rajeev, G.; Takadama, H.; Rao Bakshi, S. Fabrication of dense alumina layer on Ti alloy hybrid by cold metal transfer and micro-arc oxidation methods. *J. Mater. Res.* **2017**. [CrossRef]
104. Angadji, A.; Royle, M.; Collins, S.N.; Shelton, J.C. Influence of cup orientation on the wear performance of metal-on-metal hip replacements. *Proc. Inst. Mech. Eng. H* **2009**, *223*, 449–457. [CrossRef] [PubMed]
105. Elkins, J.M.; O'Brien, M.K.; Stroud, N.J.; Pedersen, D.R.; Callaghan, J.J.; Brown, T.D. Hard-on-hard total hip impingement causes extreme contact stress concentrations. *Clin. Orthop. Relat. Res.* **2011**, *469*, 454–463. [CrossRef] [PubMed]
106. Barrack, R.L.; Burak, C.; Skinner, H.B. Concerns about ceramics in THA. *Clin. Orthop. Relat. Res.* **2004**, *429*, 73–79. [CrossRef]
107. Langton, D.J.; Jameson, S.S.; Joyce, T.J.; Gandhi, J.N.; Sidaginamale, R.; Mereddy, P.; Lord, J.; Nargol, A.V. Accelerating failure rate of the ASR total hip replacement. *J. Bone Jt. Surg. Br.* **2011**, *93*, 1011–1106. [CrossRef] [PubMed]
108. Mao, X.; Tay, G.H.; Godbolt, D.B.; Crawford, R.W. Pseudotumor in a well-fixed metal-on-polyethylene uncemented hip arthroplasty. *J. Arthroplast.* **2012**, *27*, 493.e13–493.e17. [CrossRef] [PubMed]
109. So, K.; Kaneuji, A.; Matsumoto, T.; Matsuda, S.; Akiyama, H. Is the bone-bonding ability of a cementless total hip prosthesis enhanced by alkaline and heat treatments? *Clin. Orthop. Relat. Res.* **2013**, *471*, 3847–3855. [CrossRef] [PubMed]
110. Briggs, E.P.; Walpole, A.R.; Wilshaw, P.R.; Karlsson, M.; Palsgard, E. Formation of highly adherent nano-porous alumina on Ti-based substrates: A novel bone implant coating. *J. Mater. Sci. Mater. Med.* **2004**, *15*, 1021–1029. [CrossRef] [PubMed]
111. Varlese, F.A.; Tului, M.; Sabbadini, S.; Pellissero, F.; Sebastiani, M.; Bemporad, E. Optimized coating procedure for the protection of TiAl intermetallic alloy against high temperature oxidation. *Intermetallics* **2013**, *37*, 76–82. [CrossRef]
112. Zhang, K.; Wang, Q.M.; Sun, C.; Wang, F.H. Preparation and oxidation resistance of a crack-free Al diffusion coating on $Ti_{22}Al_{26}Nb$. *Corros. Sci.* **2007**, *49*, 3598–3609. [CrossRef]
113. Chu, M.S.; Wu, S.K. The improvement of high temperature oxidation of Ti-50Al by sputtering Al film and subsequent interdiffusion treatment. *Acta Mater.* **2003**, *51*, 3109–3120. [CrossRef]
114. Novoselova, T.; Celotto, S.; Morgan, R.; Fox, P.; O'Neill, W. Formation of TiAl intermetallics by heat treatment of cold-sprayed precursor deposits. *J. Alloy. Compd.* **2007**, *436*, 69–77. [CrossRef]
115. Balani, K.; Laha, T.; Agarwal, A.; Karthikeyan, J.; Munroe, N. Effect of carrier gases on microstructural and electrochemical behavior of cold-sprayed 1100 aluminum coating. *Surf. Coat. Technol.* **2005**, *195*, 272–279. [CrossRef]
116. Kang, K.; Won, J.; Bae, G.; Ha, S.; Lee, C. Interfacial bonding and microstructural evolution of Al in kinetic spraying. *J. Mater. Sci.* **2012**, *47*, 4649–4659. [CrossRef]

117. Yerokhin, A.L.; Nie, X.; Leyland, A.; Matthews, A.; Dowey, S.J. Plasma electrolysis for surface engineering. *Surf. Coat. Technol.* **1999**, *122*, 73–93. [CrossRef]
118. Nie, X.; Leyland, A.; Song, H.W.; Yerokhin, A.L.; Dowey, S.J.; Matthews, A. Thickness effects on the mechanical properties of micro-arc discharge oxide coatings on aluminium alloys. *Surf. Coat. Technol.* **1999**, *116*, 1055–1060. [CrossRef]
119. Sundararajan, G.; Krishna, L.R. Mechanisms underlying the formation of thick alumina coatings through the MAO coating technology. *Surf. Coat. Technol.* **2003**, *167*, 269–277. [CrossRef]
120. Hussein, R.O.; Nie, X.; Northwood, D.O. Influence of process parameters on electrolytic plasma discharging behaviour and aluminum oxide coating microstructure. *Surf. Coat. Technol.* **2010**, *205*, 1659–1667. [CrossRef]
121. Yerokhin, A.L.; Shatrov, A.; Samsonov, V.; Shashkov, P.; Pilkington, A.; Leyland, A.; Matthews, A. Oxide ceramic coatings on aluminium alloys produced by a pulsed bipolar plasma electrolytic oxidation process. *Surf. Coat. Technol.* **2005**, *199*, 150–157. [CrossRef]